Si–H Bond Activation

International Edition: DOI: 10.1002/anie.201604001
German Edition: DOI: 10.1002/ange.201604001

J(Si,H) Coupling Constants in Nonclassical Transition-Metal Silane Complexes

Wolfgang Scherer, Petra Meixner, Kilian Batke, José E. Barquera-Lozada, Klaus Ruhland, Andreas Fischer, Georg Eickerling, and Klaus Eichele*

Abstract: *We will outline that the sign and magnitude of J(Si,H) coupling constants provide a highly sensitive tool to measure the extent of Si–H bond activation in nonclassical silane complexes. Up to now, this structure–property relationship was obscured by erroneous J(Si,H) sign determinations in the literature. These new findings also help to identify the salient control parameters of the Si–H bond activation process in nonclassical silane complexes.*

Nonclassical silane complexes can be considered as arrested intermediates of the oxidative addition of a Si–H bond to a transition-metal center *M*.[1] During the early stage of this oxidative addition process, σ-silane complexes are formed, which are characterized by elongated and, thus, activated Si–H bonds, for example, in $Cr(CO)_5(\eta^2\text{-}H_2SiPh_2)$[2] (**A** in Figure 1). The terminus of this reaction coordinate is reached upon formation of classical silyl hydride species (e.g. $Fe(PMe_2Ph)(CO)_3(H)(SiPh_3)$[3] that display two-center, two-electron (2c2e) *M*–Si and *M*–H bonds (**D** in Figure 1).

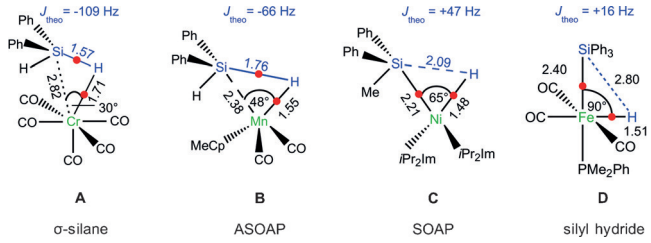

Figure 1. Salient theoretical structural parameters (distances in Å) and *J*(Si,H) spin–spin coupling constants of benchmark systems for σ-silane complexes (**A**), asymmetric and symmetric oxidative addition products (ASOAP (**B**) and SOAP (**C**), respectively), and classical silyl hydride species (**D**). Red spots denote bond critical points (BCPs).

[*] Prof. Dr. W. Scherer, M. Sc. P. Meixner, Dipl.-Phys. K. Batke, Prof. Dr. K. Ruhland, M. Sc. A. Fischer, Dr. G. Eickerling
Institut für Physik, Universität Augsburg
Universitätsstrasse 1, 86135 Augsburg (Germany)
E-mail: wolfgang.scherer@physik.uni-augsburg.de
Dr. K. Eichele
Institut für Anorg. Chemie, Universität Tübingen
Auf der Morgenstelle 18, 72076 Tübingen (Germany)
Dr. J. E. Barquera-Lozada
Instituto de Química
Universidad Nacional Autónoma de México
Ciudad Universitaria, 04510 (Mexico)
Supporting information and the ORCID identification number(s) for the author(s) of this article can be found under http://dx.doi.org/10.1002/anie.201604001.

Intermediates of this process can be considered as asymmetric and symmetric oxidative addition products (ASOAP and SOAP, respectively), which both display residual Si–H bonding interactions and 2c2e *M*–H bonds (Figure 1).[4,5] The ASOAP and SOAP complexes differ, however, in the extent of the formation of the covalent *M*–Si bond, which is still at an early stage in the first case (e.g. $Cp^{\#}Mn(CO)_2(H_2SiPh_2)$[6,7] (**B**), where $Cp^{\#} = MeCp$), but close to completion in the latter case (e.g. $Ni(iPr_2Im)_2(HSiMePh_2)$[5,8] (**C**), where iPr_2Im = 1,3-diisopropylimidazolin-2-ylidene). Numerous related nonclassical interactions have been proposed, which include α-agostic silyl complexes,[9] secondary interactions between a silicon and a hydrogen atom (SISHA),[10] and complexes displaying interligand hypervalent interactions (IHIs).[11a] Main group complexes displaying Si–H···B[11b] and Si–H···Si[11c] interactions have also been isolated in the meantime. These types of interactions are, however, beyond the scope of the current study. We have recently shown on the basis of experimental and theoretical charge density studies that nonclassical transition-metal silane species display a continuum of electronic structures along the oxidative addition reaction coordinate and can, therefore, be described by a unifying bonding concept.[4,7,12] Herein we will show that the sign and the magnitude of the *J*(Si,H) spin–spin coupling constants as well as characteristic charge density features can be employed to reveal the extent of the addition of Si–H bonds to metal atoms.

Indeed, the pioneering NMR studies by Corriou and coworkers in 1982[13] identified the magnitude of *J*(Si,H) spin–spin coupling constants as a versatile tool to analyze the Si–H bond activation process in transition-metal silane complexes. This is illustrated in Figure 1 by the calculated individual *J*(Si,H) coupling constants of our model systems **A**–**D**, which cover a rather wide range from −109 Hz (**A**) to +16 Hz (**D**) and appear to decrease systematically in magnitude as the degree of Si–H bond activation increases from **A** to **D**. At this stage of our analysis we focus on values obtained from DFT calculations,[14] since they are unbiased by solvation and crystal-packing effects and also allow a direct comparison of salient benchmark systems in cases where a time-demanding experimental determination of NMR properties (i.e. the sign of the *J*(Si,H) coupling constants) was hindered by the inherent chemical instability of the respective samples.[15] The computational study suggests that the large Si–H bond length in the silyl hydride species **D** (> 2.5 Å) is reflected by a small magnitude of the respective |*J*(Si,H)| coupling constant (< 20 Hz; Figure 1). In contrast, nonclassical silane complexes (e.g. **A**–**C** in Figure 1) form three- or multicenter bonds, where the bridging hydrido ligand interacts simultaneously

with the metal and the silicon atom. As a consequence of the residual Si–H interaction, larger $|J(\mathrm{Si,H})|$ coupling constants are predicted by DFT calculations relative to those of **D**. Since the first systematic studies of these systems by Schubert in 1990,[16] it has been proposed that bridging [*M*,H,Si] entities in nonclassical silane complexes can be identified by short Si–H bond lengths (< 2.2 Å) and $|J(\mathrm{Si,H})|$ coupling constants significantly larger than 20 Hz. However, the transition between classical and nonclassical silane complexes is a rather continuous one and is mainly controlled by the electronic influence of the substituents at the silicon atom and the local electronic situation at the transition metal.[4] Hence, the characteristic interval of $|J(\mathrm{Si,H})|$ coupling constants (20–70 Hz), which was originally proposed by Schubert[16] to identify nonclassical silane complexes with residual covalent Si–H bonds, still remains a matter of intense debate.[10]

As pointed out by Corriou and co-workers,[13] the situation is further complicated by the fact that the observed total coupling constants $J(\mathrm{Si,H}) = {}^1J(\mathrm{Si,H}) + {}^2J(\mathrm{Si},M,\mathrm{H})$ can be considered the result of two competing mechanisms, which provide coupling contributions of opposite sign to the total *J*(Si,H) values. Indeed, as a consequence of the negative gyromagnetic ratio of the ^{29}Si nucleus ($\gamma = -53.2 \times 10^6$ rads^{-1}T^{-1}), the corresponding signs of ${}^1J(\mathrm{Si,H})$ and ${}^2J(\mathrm{Si},M,\mathrm{H})$ are assumed to be negative and positive, respectively, in the simple Dirac vector model.[17] Hence, the magnitude of the observed *J*(Si,H) coupling constants might even vanish if both coupling components are of equal magnitude and cancel each other out. Therefore, the magnitude of the *J*(Si,H) coupling constants alone cannot be taken as a measure of the σ(Si-H) interaction strength[18a] and it is, therefore, essential to also determine the sign of the *J*(Si,H) coupling constant.

According to Ignatov et al., only a negative sign of *J*(Si,H) should provide "conclusive evidence of the presence of a direct Si–H bond"[18a] and signals the predominance of the ${}^1J(\mathrm{Si,H})$ contribution. On the basis of this simple criterion, the asymmetric and symmetric oxidative addition products **B** and **C** can be clearly differentiated, since only **B** is characterized by a negative *J*(Si,H) coupling constant (−66 Hz), which suggests a predominant ${}^1J(\mathrm{Si,H})$ coupling character and, thus, the presence of a highly activated, but still covalent, Si–H bond. In contrast, **C** displays a positive *J*(Si,H) value of +47 Hz and can be classified as a symmetric oxidation addition product since the Ni–Si and Ni–H bond-formation process is almost complete, which implies that the ${}^2J(\mathrm{Si},M,\mathrm{H})$ coupling mechanism dominates. As a consequence, the Si–H bond in **C** is nearly broken, as signaled by the large Si–H bond length of 2.09 Å and the lack of a Si–H bond critical point (BCP) in combined experimental and theoretical charge density analyses.[5] The acute ∠(Si,Ni,H) valence angle of 65° alone hints at best for elusive, residual Si···H bonding interactions in **C**. In the case of **B**, however, a Si–H BCP exists, but the density accumulation at the BCP is still small ($\rho(\mathbf{r}) = 0.56$ e Å^{-3}) compared to the σ-silane species **A** ($\rho(\mathbf{r}) = 0.66$ e Å^{-3}). The latter species is characterized by a covalent Si–H bond (d(Si-H) = 1.57 Å) that is activated relative to the unperturbed covalent Si–H bond in uncoordinated SiH_4 (1.4798(4) Å).[19] Hence, only **A** and **D** represent clear-cut benchmark systems in which either the ${}^1J(\mathrm{Si,H})$ (in **A**) or the ${}^2J(\mathrm{Si},M,\mathrm{H})$ coupling scenario (in **D**) dominate the *J*(Si,H) coupling constants because of the presence or absence of covalent Si–H bonds, respectively. The nonclassical silanes **B** and **C**, thus, represent intermediate cases.

Since all the models **A**–**D** can be classified by their charge density topology as well as their *J*(Si,H) values, we were interested in exploring whether nonclassical silanes displaying electronegative chlorine substituents can be grouped in the same way. We outlined previously that electronegative substituents *X* at the silicon atoms in a *trans* position with respect to the bridging η(Si-H) entities enhance the $M \rightarrow \sigma^*$(H-Si-*X*) π back-donation, which again leads to an increase in the *M*–Si bond strength in early transition-metal silane complexes such as $Cp_2Ti(PMe_3)(HSiMe_{3-n}Cl_n)$ ($n = 0$–3) **1a**–**1d** and $Cp_2Ti(PMe_3)(HSiHPhCl)$[15a] **1b′** (Figures 2–4).[4] In the charge density picture, the enhancement of the *M*–Si bond strength leads to an increasing density at the Si–*M* BCP with an increasing number of chlorine substituents in **1a**–**1d**. The same situation holds in the case of the Schubert-type manganese complexes. Here, a Si–*M* BCP is lacking in model **B** (Figure 1), but forms in the complex $(Cp^{\#})Mn(CO)_2(HSiFPh_2)$ (**B′**), which has a fluorine substituent in the *trans* position to the η^1(Si-H) moiety.[7,12] This observation is again in line with an enhanced $M \rightarrow \sigma^*$(H-Si-*X*) π back-donation in **B′** relative to **B**. The simultaneous presence of the *M*–Si, Si–H, and *M*–H BCPs in the benchmark systems **1a**–**1d** might, therefore, hint at an intermediate electronic situation between the scenarios displayed by **B** and **C**.

Indeed, the theoretical *J*(Si,H) coupling constants of **1a**–**1d** change their signs from negative (**1a**) to positive (**1d**) as the number of chlorine substituents increases, which simultaneously reduces the Ti–Si bond length and enhances the completion of the oxidative addition process (Figure 2). Note that the Ti–H bond lengths of complexes **1a**–**1d** are virtually identical, since the Ti–H bond-formation process in these asymmetric oxidative addition products is already nearly completed. The Si–H bond lengths and the ∠(Si,Ti,H) valence angle do not provide a good measure of the extent of the oxidative addition process in **1a**–**1d**, since metal-mediated Si–H as well as C–H bond-activation processes are mainly controlled by the presence and extent of a local Lewis-acidic site at the metal center[20a–d] in analogy with a vacant d orbital in the MO picture.[20e] As we concluded in a previous study, "*the spatial extent of this local Lewis-acidic center is fundamentally linked with the size of the d-orbitals involved in the $M \rightarrow \sigma^*$(X-Si-H) π back donation*" and, therefore, rather invariant in **1a**–**1d**.[4]

These clear trends in the theoretical *J*(Si,H) coupling constants of **1a**–**1d** are, however, at first glance in conflict with the corresponding values determined by Ignatov et al. by spin tickling experiments.[18a] This experimental study proposed negative *J*(Si,H) values of −22 Hz and −34 Hz for the nonclassical titanium silane complexes **1c** and **1d**, respectively, which are at clear variance with our theoretical predictions (+34 Hz (**1c**), +58 Hz (**1d**); Figure 2 and Ref. [5]). These findings let Ignatov et al. conclude that **1c** and **1d** are characterized by covalent Si–H bonds, and the authors coined the expression interligand hypervalent inter-

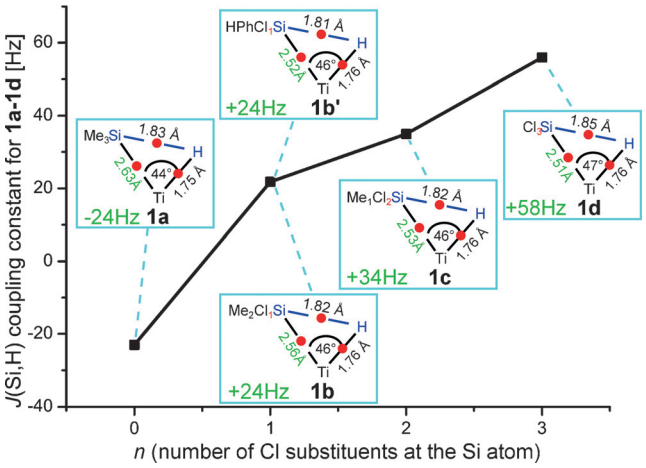

Figure 2. Influence of electronegative chlorine substituents on the calculated J(Si,H) coupling constants and Ti–Si bond length in the metal complexes $Cp_2Ti(PMe_3)(HSiMe_{3-n}Cl_n)$ **1a**–**1d** and $Cp_2Ti(PMe_3)$-(HSiHPhCl) **1b′**. Red spots denote bond critical points (BCPs). See S4 in the Supporting Information for more detailed information. Only coupling contributions from the Fermi contact (FC) spin–spin coupling mechanism are considered. These values change marginally ($< \pm 2$ Hz) when the spin–dipole, paramagnetic orbital, and diamagnetic orbital terms are also included.

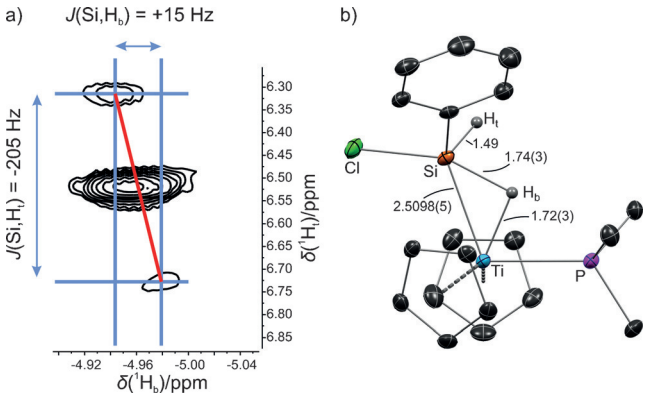

Figure 3. a) Section of the 500 MHz ^{1}H-^{1}H-COSY spectrum of **1b′** (Ref. [15a]). The red solid line interconnects the centers of the two ^{29}Si satellites next to the ^{1}H signal of the bridging Ti-H_b-Si moiety. From its negative slope, one can conclude that the individual $^1J(Si,H_t)$ and $J(Si,H_b)$ coupling constants are of opposite sign (Ref. [15c]). Since $^1J(Si,H_t) < 0$ (Ref. [17]), the sign of $J(Si,H_b)$ must be positive (+15 Hz), in line with the DFT predictions (+24 Hz). b) ORTEP representation (ellipsoids set at 50% probability) of **1b′** at 100(2) K (Ref. [15d]). Salient bond distances are specified in Å and only hydrogen atoms attached to the silicon atom are drawn.

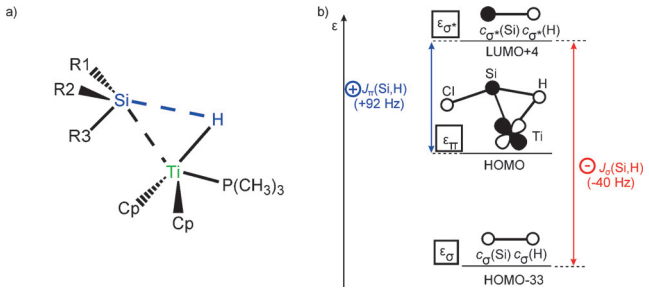

Figure 4. a) Nonclassical silane complexes **1a**–**1d**. **1a**: R1 = R2 = R3 = Me; **1b**: R1 = R2 = Me, R3 = Cl; **1c**: R1 = Me, R2 = R3 = Cl; **1d**: R1 = R2 = R3 = Cl; **1b′**: R1 = H, R2 = Ph, R3 = Cl. b) Schematic representation of the decomposition of the J(Si,H) coupling constant of $Cp_2Ti(PMe_3)(HSiCl_3)$ (**1d**) into individual J_σ(Si,H) and J_π(Si,H) contributions from pairs of interacting occupied and virtual MOs. Only major orbital interactions contributing to the Fermi contact terms are considered. See Table 1 and the Supporting Information for a detailed analysis.

actions (IHIs)[18] as the bonding scenario for **1b**–**1d**. However, **1c** and **1d** appear to be rather unsuitable benchmark systems for an unequivocal determination of the sign of J(Si,H) (see the Supporting Information for further details). We, therefore, decided to synthesize $Cp_2Ti(PMe_3)(H_bSiH_tPhCl)$ (**1b′**), which is electronically closely related to our benchmark systems **1b**–**1d**. **1b′** displays a noncoordinating *terminal* Si–H_t moiety characterized by a negative $^1J(Si,H_t)$ coupling constant, which can be used as an internal reference for an unequivocal sign determination of $J(Si,H_b)$ of the *bridging* Si–H_b group. Indeed, analysis of the individual J coupling contributions to the cross-peak multiplet of the three-spin system (^1H_t, ^1H_b, ^{29}Si; Figure 3) finally allowed determination of the sign of $J(Si,H_b)_{exp}$ (+15 Hz) in the case of **1b′**, which is in agreement with the DFT predictions (+24 Hz; Figure 2).

To clarify which electronic control parameters determine the sign of J(Si,H) coupling constants in nonclassical silane complexes we also analyzed the individual molecular orbital (MO) contribution to the isotropic coupling resulting from the Fermi-contact mechanism. In these studies, we used a density functional method[14] developed by Ziegler and Autschbach[21] for the analytic calculation of nuclear spin–spin coupling constants which employs the relativistic zeroth-order regular approximation (ZORA).[22] With this approach, it is also possible to decompose the J(Si,H) coupling constants of our benchmark systems into individual contributions from pairs of interacting occupied and virtual MOs. This is illustrated schematically in Figure 4 for the case of the Ti complex **1d**.

Note that the HOMO in Figure 4 represents a Ti→σ^*(H-Si-Cl) π back-donation and HOMO-33 the σ(Si-H) bonding orbital of **1d**. The corresponding coupling contributions from the mixing of HOMO and HOMO-33 with the vacant σ^*(Si-H) orbital (LUMO + 4) have been denoted J_π(Si,H) and J_σ(Si,H), respectively. In the following, we will employ approximation (1)[23] to determine the sign of the J_π(Si,H) and J_σ(Si,H) coupling contributions.

$$J_{\sigma/\pi}(\mathrm{Si,H}) \sim (-1) \times \mathrm{const} \times [c_o(\mathrm{Si})c_v(\mathrm{Si}) \times c_o(\mathrm{H})c_v(\mathrm{H})]/(\varepsilon_o - \varepsilon_v) \quad (1)$$

In approximation (1), $c_o(X)$ and $c_v(X)$ (X = Si or H) are the coefficients of the atomic orbitals of the silicon and hydrogen atom in the occupied and virtual MO, respectively. The negative prefactor (−1) in approximation (1) considers the negative gyromagnetic ratio of the silicon atom. In the case of the mixing of HOMO-33 and LUMO + 4, the orbital overlap term $[c_o(\mathrm{Si})c_v(\mathrm{Si}) \times c_o(\mathrm{H})c_v(\mathrm{H})]$ and the energy difference term $(\varepsilon_o - \varepsilon_v)$ are both negative. The resulting coupling constant (denoted J_σ(Si-H) in Figure 4) is negative—provided

the Fermi contact mechanism is the dominant one.

This is actually the case for all model systems (**1a**–**1d**, **1b**′) considered in this study (Table 1). In the same way, the mixing of HOMO and LUMO + 4 yields a positive coupling contribution (denoted J_π(Si,H) in Figure 4). The positive sign of J_π(Si,H) is a direct consequence of the presence of a nodal plane in the Ti→σ*(H-Si-Cl) bonding orbital (HOMO) yielding a positive numerator in approximation (1). More detailed DFT calculations show that the sum of the components J_π(Si,H) (+92 Hz) and J_σ(Si,H) (−40 Hz) already yields a value of +52 Hz, which is close to the total J(Si,H) coupling constant of +58 Hz for **1d** (see Table 1 for a more detailed analysis). Accordingly, the interplay of the J_π(Si,H) and J_σ(Si,H) components in the MO model of transition-metal silane complexes might play a similar role as the ^1J(Si,H) and ^2J(Si,M,H) components in the classical picture (see above). However, we wish to point out that, already at this stage, the terms ^1J(Si,H) and ^2J(Si,M,H) are poorly defined in the case of the delocalized electronic structures established by the [Si,M,H] entities in transition-metal silane complexes. We will, therefore, probe the more sophisticated MO model and clarify whether it provides a direct linkage between J(Si,H) coupling constants and the progress of the oxidative addition of Si–H bonds to metal atoms.

Table 1: Contributions to the Fermi contact term J(Si,H) from the mixing of occupied and virtual orbitals in **1a**–**1d** and **1b**′

J(Si,H) [Hz]	**1a**	**1b**	**1b**′	**1c**	**1d**
$J_{\sigma,\text{total}}$(Si,H)	−67	−58	−50	−64	−65[a]
$J_{\pi,\text{total}}$(Si,H)	+51	+71	+72	+99	+144[a]
remaining orbital interactions	−8	+11	+2	−1	−21
all FC terms	−24	+24	+24	+34	+58

[a] Note that in Figure 4, only the MO interactions with one single virtual MO (LUMO + 4) have been considered.

In the next step we have, therefore, analyzed whether the J_π(Si,H) and J_σ(Si,H) coupling contributions also determine the sign and magnitude of the J(Si,H) coupling constants for the remaining members of the **1a**–**1d** series. For this purpose we will consider all coupling contributions emerging from the interactions between the occupied σ(Si-H) and Ti→σ*(H-Si-Cl) orbitals with the complete set of virtual orbitals. These interactions will be denoted $J_{\pi,\text{total}}$(Si,H) and $J_{\sigma,\text{total}}$(Si,H) in the following. We learn from Table 1 that the $J_{\sigma,\text{total}}$(Si,H) coupling contributions remain rather constant and do not change significantly when the number of chlorine substituents is reduced (−65 Hz (**1d**, n = 3); −64 Hz (**1c**, n = 2); −58 Hz (**1b**, n = 1); −67 Hz (**1a**, n = 0)). The rather constant coupling contributions arising from these MO interactions might be connected with the trends observed in structural and charge density studies. As explained above, the Si–H bond lengths in **1a**–**d** are rather independent of the individual degree of substitution n (1.848 Å in **1d** (n = 3); 1.822 Å in **1c** (n = 2); 1.822/1.808 Å in **1b**/**1b**′ (n = 1); and 1.826 Å in **1a** (n = 0)), and the charge density at the Si–H bond critical points also remains rather constant (0.51 e Å^{-3} in **1d** (n = 3); 0.52 e Å^{-3} in **1c** (n = 2); 0.50/0.52 e Å^{-3} in **1b**/**1b**′ (n = 1); and 0.50 e Å^{-3} in **1a** (n = 0)). Hence, the insignificant changes in the Si–H bonding and activation in the series **1a**–**1d** is reflected by their rather constant $J_{\sigma,\text{total}}$(Si,H) coupling parameters.

A rather different trend is, however, evident from Table 1 for the $J_{\pi,\text{total}}$(Si,H) interactions. This is manifested in the sharp increase in the $J_{\pi,\text{total}}$(Si,H)-type contributions to the J(Si,H) coupling constants upon an increase in the degree of substitution n (+51 Hz in **1a** (n = 0); +71 Hz in **1b** (n = 1); +99 Hz in **1c** (n = 2); +144 Hz in **1d** (n = 3)). The degree of oxidative addition, which increases as the Ti→σ*(H-Si-Cl) π back-donation increases, appears to be reflected by increasing $J_{\pi,\text{total}}$(Si,H) coupling contributions. Hence, the trend of the total J(Si,H) coupling constants as displayed in Figure 2 might be explained simply by inspection of the individual negative $J_{\sigma,\text{total}}$(Si,H)-type and positive $J_{\pi,\text{total}}$(Si,H)-type contributions alone.

In summary, a simple structure–property relationship emerges from our study: The positive sign of J(Si,H) coupling constants in the series of $Cp_2Ti(PMe_3)(HSiMe_{3-n}Cl_n)$ (with n = 1–3) **1b**–**1d** is due to the increase in the J_π(Si,H) coupling contributions which emerge from the increasing dominance of the Ti→σ*(H-Si-Cl) π back-donation between the metal and the silane ligand as the number of electron-withdrawing ligands at the silicon atom increases.[4,7,12] This trend does not depend on the presence of additional IHI interactions, which would be characterized by a pronounced σ(Ti-H)/σ*(Si-Cl) orbital interaction mechanism. According to our DFT studies, the latter interaction provides (if at all) only a minor coupling contribution (< 3 Hz) to the total J(Si,H) coupling constants and, in contrast to earlier suggestions,[18b] can be safely ignored.

Acknowledgements

This work was supported by the DFG (SPP1178) project number SCHE478/9-3. J.E.B.-L. acknowledges DGSCA, UNAM, for supercomputer time through project SC15-1-IR-66.

Keywords: charge density · coupling constants · MO analysis · NMR spectroscopy · nonclassical silane complexes

How to cite: *Angew. Chem. Int. Ed.* **2016**, *55*, 11673–11677
Angew. Chem. **2016**, *128*, 11846–11850

[1] J. Y. Corey, *Chem. Rev.* **2011**, *111*, 863–1071.
[2] S. L. Matthews, V. Pons, D. M. Heinekey, *Inorg. Chem.* **2006**, *45*, 6453–6459.
[3] H. Li, L. C. Misal Castro, J. Zheng, T. Roinel, V. Dorcet, J.-B. Sortais, C. Darcel, *Angew. Chem. Int. Ed.* **2013**, *52*, 8045–8049; *Angew. Chem.* **2013**, *125*, 8203–8207.
[4] W. Scherer, P. Meixner, J. E. Barquera-Lozada, C. Hauf, A. Obenhuber, A. Brück, D. J. Wolstenholme, K. Ruhland, D. Leusser, D. Stalke, *Angew. Chem. Int. Ed.* **2013**, *52*, 6092–6096; *Angew. Chem.* **2013**, *125*, 6208–6212.
[5] C. Hauf, J. E. Barquera-Lozada, P. Meixner, G. Eickerling, S. Altmannshofer, D. Stalke, T. Zell, D. Schmidt, U. Radius, W. Scherer, *Z. Anorg. Allg. Chem.* **2013**, *639*, 1996–2004.
[6] U. Schubert, K. Ackermann, B. Wörle, *J. Am. Chem. Soc.* **1982**, *104*, 7378–7380.

[7] W. Scherer, G. Eickerling, M. Tafipolsky, G. S. McGrady, P. Sirsch, N. P. Chatterton, *Chem. Commun.* **2006**, 2986 – 2988.
[8] T. Zell, T. Schaub, K. Radacki, U. Radius, *Dalton Trans.* **2011**, *40*, 1852 – 1854.
[9] A. D. Sadow, T. D. Tilley, *J. Am. Chem. Soc.* **2003**, *125*, 9462 – 9475.
[10] a) S. Lachaize, S. Sabo-Etienne, *Eur. J. Inorg. Chem.* **2006**, 2115 – 2127; b) K. A. Smart, M. Grellier, Y. Coppel, L. Vendier, S. A. Mason, S. C. Capelli, A. Albinati, V. Montiel-Palma, M. A. Muñoz-Hernández, S. Sabo-Etienne, *Inorg. Chem.* **2014**, *53*, 1156 – 1165.
[11] a) G. I. Nikonov, *Adv. Organomet. Chem.* **2005**, *53*, 217 – 309; b) A. Y. Houghton, J. Hurmalainen, A. Mansikkamäki, W. E. Piers, H. M. Tuononen, *Nat. Chem.* **2014**, *6*, 983 – 988; c) S. P. Hoffmann, T. Kato, F. S. Tham, C. A. Reed, *Chem. Commun.* **2006**, 767 – 769.
[12] G. S. McGrady, P. Sirsch, N. P. Chatterton, A. Ostermann, C. Gatti, S. Altmannshofer, V. Herz, G. Eickerling, W. Scherer, *Inorg. Chem.* **2009**, *48*, 1588 – 1598.
[13] E. Colomer, R. J. P. Corriu, C. Marzin, A. Vioux, *Inorg. Chem.* **1982**, *21*, 368 – 373.
[14] All DFT calculations were performed with ADF using the PBE0 functional, the ZORA for the description of scalar relativistic effects, and the TZ2P or JCPL basis set as implemented in ADF; see the Supporting Information for further details.
[15] a) Compounds **1b′**, **1c**, and **1d** were synthesized according to a slightly modified literature procedure (Ref. [18a]). The corresponding hydrosilane was added to the complex $Cp_2Ti(PMe_3)_2$ in a mixture of toluene/hexane (1:3 for **1b′** and 3:2 for **1d**). b) The 2D NMR measurements were performed on a Bruker Avance II + 500 at the University of Tübingen. c) J. Keeler in *Understanding NMR Spectroscopy*, Wiley, New York, **2010**, p. 334. d) Crystal data for **1b′**: $M_r = 396.81$, 100(2) K with $Ag_{K\alpha}$ radiation ($\lambda = 0.56087$ Å): monoclinic, space group $P2_1/n$, $a = 8.5194(5)$, $b = 15.4060(8)$, $c = 15.2989(8)$ Å, $\beta = 98.187(2)°$, $V = 1987.5(2)$ Å^3, $Z = 4$, $\rho_{calcd} = 1.326\ g\,cm^{-3}$, $\mu = 0.36\ mm^{-1}$ for a total of 28081 reflections yielding 4495 unique reflections ($R_{int} = 0.0494$, 98.6% completeness for $1.488 < \theta < 21.373°$). Refinements of 219 parameters converged to $R1 = 0.0355$ and $wR2 = 0.0825$. CCDC 1476700 contains the supplementary crystallographic data for this paper. These data can be obtained free of charge from The Cambridge Crystallographic Data Centre via www.ccdc.cam.ac.uk/data_request/cif.
[16] U. Schubert, *Adv. Organomet. Chem.* **1990**, *30*, 151 – 187.
[17] J. Schraml, J. M. Bellama in *Determination of Organic Structures by Physical Methods*, *Vol. 6* (Eds.: F. C. Nachod, J. J. Zuckerman, E. W. Randall), Academic Press, New York, **1976**, pp. 203 – 269.
[18] a) S. K. Ignatov, N. H. Rees, B. R. Tyrrell, S. R. Dubberley, A. G. Razuvaev, P. Mountford, G. I. Nikonov, *Chem. Eur. J.* **2004**, *10*, 4991 – 4999; b) The IHI bonding scenario is defined in terms of a hyperconjugative electron donation from a σ(*M*-H) orbital into an antibonding σ*(Si-*X*) orbital of a metal-coordinating silane ligand, as detailed in Ref. [18a].
[19] D. R. J. Boyd, *J. Chem. Phys.* **1955**, *23*, 922 – 926.
[20] a) W. Scherer, G. S. McGrady, *Angew. Chem. Int. Ed.* **2004**, *43*, 1782 – 1806; *Angew. Chem.* **2004**, *116*, 1816 – 1842; b) W. Scherer, V. Herz, A. Brück, C. Hauf, F. Reiner, S. Altmannshofer, D. Leusser, D. Stalke, *Angew. Chem. Int. Ed.* **2011**, *50*, 2845 – 2849; *Angew. Chem.* **2011**, *123*, 2897 – 2902; c) W. Scherer, V. Herz, C. Hauf, *Struct. Bonding* **2012**, *146*, 159 – 207; d) W. Scherer, D. J. Wolstenholme, V. Herz, G. Eickerling, A. Brück, P. Benndorf, P. W. Roesky, *Angew. Chem. Int. Ed.* **2010**, *49*, 2242 – 2246; *Angew. Chem.* **2010**, *122*, 2291 – 2295; e) R. F. W. Bader, C. F. Matta, F. Cortés-Guzmán, *Organometallics* **2004**, *23*, 6253 – 6263.
[21] a) J. Autschbach, T. Ziegler, *J. Chem. Phys.* **2000**, *113*, 936 – 947; b) J. Autschbach, T. Ziegler, *J. Chem. Phys.* **2000**, *113*, 9410 – 9418.
[22] E. van Lenthe, E. J. Baerends, J. G. Snijders, *J. Chem. Phys.* **1993**, *99*, 4597 – 4610.
[23] a) J. A. Pople, A. A. Bothner-By, *J. Chem. Phys.* **1965**, *42*, 1339 – 1349; b) J. Autschbach, B. le Guennic, *J. Chem. Educ.* **2007**, *84*, 156 – 171.

Received: April 25, 2016
Revised: May 31, 2016
Published online: August 9, 2016

